Sodium Currents during Differentiation in a Human Neuroblastoma Cell Line

RICHARD E. WEISS and NEIL SIDELL

From the Ahmanson Neurobiology Laboratory and the Departments of Pediatric Cardiology and Pathology, University of California, Los Angeles School of Medicine, Los Angeles, California 90024

ABSTRACT   The electrophysiological properties of a human neuroblastoma cell line, LA-N-5, were studied with the whole-cell configuration of the patch clamp technique before and after the induction of differentiation by retinoic acid, a vitamin A metabolite. Action potentials could be elicited from current clamped cells before the induction of differentiation, suggesting that some neuroblasts of the developing sympathetic nervous system are excitable. The action potential upstroke was carried by a sodium conductance, which was composed of two types of sodium currents, described by their sensitivity to tetrodotoxin (TTX) as TTX sensitive and TTX resistant. TTX-sensitive and TTX-resistant sodium currents were blocked by nanomolar and micromolar concentrations of TTX, respectively. The voltage sensitivity of activation and inactivation of TTX-resistant sodium current is shifted -10 to -30 mV relative to TTX-sensitive sodium current, suggesting that TTX-resistant sodium current could play a role in the initiation of action potentials. TTX-sensitive current comprised $>80\%$ of the total sodium current in undifferentiated LA-N-5 cells. The surface density of total sodium current increased from 24.9 to 57.8 $\mu A/\mu F$ after cells were induced to differentiate. The increase in total sodium current density was significant ($P < 0.05$). The surface density of TTX-resistant sodium current did not change significantly during differentiation, from which we conclude that an increase in TTX-sensitive sodium current underlies the increase in total current.

INTRODUCTION

Sodium channels are essential to the electrical activity of nearly all excitable cells, yet relatively little is known about when they appear during development and which types appear first. Diversity among sodium channels is known to exist in mammalian nerve and muscle based on cDNA and amino acid sequences, protein subunit composition, and pharmacological and physiological properties (for review, see Ritchie and Rogart, 1977; Catterall, 1986; Barchi, 1988; Trimmer and Agnew, 1989). Significant functional differences in channel properties within the same cell type have been described so far in mammalian muscle cells between two classes of sodium

channels distinguished by affinities for tetrodotoxin (TTX) in the nanomolar (TTX sensitive) and micromolar (TTX resistant) concentration ranges (Pappone, 1980; Weiss and Horn, 1986a, b; Gonoi et al., 1989). In several types of neuronal cells where no differences in toxin sensitivity were detected, sodium currents have also separated into components with different properties (Llinas and Sugimori, 1980; Gilly and Armstrong, 1984; French and Gage, 1985; Kojima et al., 1985). It has been proposed that TTX-resistant sodium channels and several of the TTX-sensitive subtypes of sodium channels have a role in triggering spontaneous action potentials or facilitating the early depolarization phase of action potentials.

Neuroblastoma cell lines, derived from precursors of the sympathetic autonomic nervous system, respond to a variety of agents by ceasing proliferation and acquiring many characteristics of adult neurons (for review, see Kimhi, 1981). It is also believed that many of the characteristics of normal neuroblasts and ganglion cells are retained in the corresponding tumor cells based on anatomical and histochemical evidence (Kimhi, 1981; Machin, 1982). Because they can be cloned to provide homogeneous populations, neuroblastomas are especially useful as models of neuronal differentiation. The development of the patch clamp technique has now made possible studies of ion channels in neuroblastoma cells that were too small to voltage clamp by other methods. Previous investigations of excitability in undifferentiated murine neuroblastoma cell lines have shown that many cells can generate sodium-dependent action potentials, and that cell resting potentials and action currents increase with differentiation (Nelson et al., 1971; Peacock et al., 1972). The rat pheochromocytoma cell line PC12, derived originally from the neural crest (as are neuroblastomas), has also been used as a model for neuronal differentiation because it acquires many adult neuronal characteristics in response to nerve growth factor (NGF), including increased expression of TTX-sensitive sodium channels and the appearance of TTX-resistant sodium channels (Dichter et al., 1977; Rudy et al., 1982, 1987; O'Lague et al., 1985). Unlike many of the neuroblastomas, PC12 cells are inexcitable before treatment with differentiating agents.

We have investigated the electrophysiology of the human neuroblastoma cell line, LA-N-5. In the presence of retinoic acid (a vitamin A metabolite), these neuroblast-derived tumor cells undergo dramatic morphological and biochemical changes which appear very similar to the transformations of normal, differentiating sympathetic neurons (Sidell et al., 1984; Robson and Sidell, 1985). LA-N-5 cells show only partial responses to NGF (Sonnenfeld and Ishi, 1982), however, which suggests that retinoic acid and NGF activate alternative pathways to promote differentiation in different neuronal tissues. A previous study of LA-N-5 cells suggested that sodium and potassium channels are the principal current carriers and that sodium current increases with differentiation (Sidell and Horn, 1985). Here we report that these cells have a sufficient density of sodium channels to be electrically excitable before differentiation. We also show that the sodium current has TTX-sensitive and TTX-resistant components which are also distinguished by different voltage sensitivities of activation and inactivation. After differentiation of LA-N-5 cells by retinoic acid, there is significant increase in the TTX-sensitive, but not the TTX-resistant, current density.

A preliminary account of some aspects of this work has been reported previously (Weiss and Sidell, 1989).

METHODS

Cell Culture and General Techniques

LA-N-5 cells were obtained through the generosity of Dr. R. C. Seeger, Childrens Hospital of Los Angeles, Los Angeles, CA. The cell culture methods used here have been previously described in detail (Sidell et al., 1984). Cultures were maintained and subcultured in RPMI-1640 medium supplemented with 10% heat-inactivated fetal calf serum, 50 IU/ml penicillin, 50 µg/ml streptomycin, and 1 µg/ml amphotericin B (Fungizone) in a 5% CO_2, 37°C incubator. Experiments were performed on cells from untreated maintenance cultures (undifferentiated), or on cells induced to differentiate with 4×10^{-6} M retinoic acid and 10^{-3} M dibutyryl cyclic AMP, or 4×10^{-6} M retinoic acid alone, as previously described (Robson and Sidell, 1985). Differentiated cultures were used 10–20 d after treatment. Cells were dislodged from their flasks by shaking and pipetted into a perfusable 0.12-ml chamber on a Zeiss Axiovert microscope (Carl Zeiss, Inc., San Leandro, CA) equipped with differential interference contrast optics. After a 20-min wait at room temperature for the cells to adhere to the bottom of the recording chamber, the bath temperature was cooled to 18.0°C (±0.3°C) by means of a Peltier temperature controller. Unless otherwise stated, all experiments were performed at 18°C.

TABLE I

Mean Currents and Current Ratios

	Undifferentiated	Differentiated
$I_{Na,Total}$, pA	290 ± 330 (71)	1,040 ± 661 (15)
$I_{Na,Total}$, µA/µF	24.9 ± 23.3 (6)	57.8 ± 28.0 (7)
$I_{Na,TTX-R}$, pA	55.7 ± 43 (24)	103 ± 118 (19)
$I_{Na,TTX-R}$, µA/µF	4.5 ± 3.0 (4)	5.1 ± 3.5 (12)
$I_{Na,TTX-R}/I_{Na,Total}$	0.15 ± 0.09 (15)	0.09 ± 0.04 (11)
Capacitance, µA/µF	20.0 ± 6.8 (7)	24.1 ± 7.4 (13)

Mean sodium currents and current ratios from undifferentiated and differentiated LA-N-5 cells. Values are given as mean ± SD with the number of samples in parentheses. The subscript TTX-R refers to TTX-resistant current measured in the presence of 160 nM TTX.

LA-N-5 cells are typically round or oval shaped, with apparent diameters of 10–25 µm and few processes. After retinoic acid–induced differentiation, apparent cell diameters were 15–35 µm for the cells used in this study, and there were typically several processes and neurites extended. Undifferentiated cells were selected for larger size and differentiated cells for smaller size and fewest extensions to afford better voltage control and comparison of results. The mean cell capacitances shown in Table I indicate that the differentiated cells selected were only slightly larger on average than the undifferentiated cells. Large differentiated cells with many extensions could not be adequately voltage clamped and were omitted from the data pool. It is possible that the selection of smaller differentiated cells may have introduced a bias into the data of sodium current magnitude and density in differentiated cells toward smaller values. However, such a bias would result in underestimation of the mean sodium current in the population, which would not change qualitatively the nature of any of the results reported here.

Data Acquisition and Analysis

The whole-cell configuration of the patch clamp technique was used to record ionic currents. For membrane voltage measurements a whole-cell configuration was first achieved, after which the patch clamp amplifier was switched to current clamp mode. Experiments were performed

using a List EPC-7 (Medical Systems Corp., Great Neck, NY) or a Dagan 3900 (DAGAN Corp., Minneapolis, MN) patch clamp amplifier. The patch clamp output was filtered at 5–10 kHz with an 8-pole Bessel filter (Frequency Devices, Haverhill, MA) for experiments with the EPC-7 amplifier, or the 4-pole Bessel filter built into the Dagan 3900 amplifier. Records were digitized at 7–12 μs/point by an Axolab-1 AD/DA interface (Axon Instruments, Inc., Foster City, CA) and stored on the hard disk of an AT-type computer. Pipettes with resistances from 1.5 to 3 mΩ and from 5 to 8 mΩ were used for voltage clamp and current clamp experiments, respectively. Voltage clamp pulse protocols to assay sodium currents involved holding the cells at −70 or −80 mV and stepping the membrane voltage through a 50-ms prepulse to −100 or −110 mV, followed by a test pulse to −10 or 0 mV. Cells were pulsed at a rate of 0.33 pulses/s. Linear leakage currents and capacity transients were subtracted on-line with scaled pulse (P/−4) routines. Series resistance compensation of 30–60% was regularly used. Data acquisition and analysis was performed using software developed by Dr. F. Bezanilla, Department of Physiology, UCLA.

Cell capacitance was estimated by measuring the difference between the areas of current transients recorded in response to 10-mV test pulses just before and after breaking into a cell (whole-cell configuration). These values were compared with a calibration curve obtained with 10-mV voltage pulses through a model membrane with various known capacitors to obtain values for actual cell capacitances. Normalized currents are expressed as μA/μF and it is assumed that the specific capacitance of the membrane is 1 μF/cm^2.

Inhibition of sodium currents by TTX was analyzed by a noncooperative, two-site model fit to the dose–response data by a nonlinear, least-squares fitting routine according to the equation

$$I = (I_{max} - I_{TR,max})*K_{d,TS}/(K_{d,TS} + [TTX]) + I_{TR,max}*K_{d,TR}/(K_{d,TR} + [TTX]) \qquad (1)$$

where I_{max} and I are, respectively, the sodium current measured in the absence and presence of the experimental dose of TTX, and $I_{TR,max}$ is the maximum TTX-resistant sodium current. $K_{d,TS}$ and $K_{d,TR}$ are, respectively, the equilibrium dissociation constants of TTX-sensitive and TTX-resistant sodium channels for TTX. $I_{TR,max}$, $K_{d,TS}$, and $K_{d,TR}$ were determined by the fitting routine.

The statistical significance of differences between mean currents of undifferentiated and differentiated LA-N-5 cells was determined by the Wilcoxon's rank sum test (Hill, 1937; Diem and Lentner, 1970). This test was selected because of the nonnormal distribution of the sodium current values (see Fig. 7 B). For comparison, the data were also analyzed by Student's t test, which applies to normal distributions. Student's t test gave similar significance levels to the rank-sum test for the differences between current magnitudes and densities of both TTX-sensitive and TTX-resistant sodium currents before and after differentiation. An additional concern regarding statistical analysis was that sodium current levels might vary with the number of cell passages. This was examined by linear regression analysis of plots of mean current values versus passage number. There were no consistent trends within 95% confidence levels. A similar concern was whether differentiation induced by retinoic acid treatment with or without cyclic AMP affected the recorded sodium currents. There was no statistical difference between the two groups, however, and therefore all data from differentiated cells were pooled.

Solutions and Channel Blockers

Three pipette solutions were used. Their names and compositions were (in mM): potassium solution 1: 140 K, 2 Mg, 0.1 Ca, 142 Cl, 1.1 EGTA, 10 HEPES, pH 7.2; potassium solution 2: 140 K, 10 Na, 1 Mg, 1 Ca, 93 Cl, 12 EGTA, 10 MgATP, pH 7.1; and cesium solution: 146 Cs, 10 Na, 1 Mg, 1 Ca, 144 Cl, 12 EGTA, 2 MgATP, 10 HEPES, pH 7.2. Potassium solution 1 was used for current clamp experiments. Potassium solution 2 and cesium solution were used for voltage clamp experiments. The bath solution used in all experiments was composed of (in

mM): 143 NaCl, 2 KCl, 1 $MgCl_2$, 2 $CaCl_2$, 10 HEPES, 6 glucose, pH 7.3. Lyophilized TTX (Calbiochem Corp., San Diego, CA) was mixed with distilled water to a stock concentration of 3 mM and diluted to its final concentration in bath solution. TTX-containing solutions were stored in 3-ml aliquots at $-20°C$ until just before use. Tetraethylammonium (TEA) was added from a 1.0 M stock solution to the bathing solution just before use.

RESULTS

Electrical Excitability

LA-N-5 cells are electrically excitable before induction of differentiation by retinoic acid. Cells were found to have resting potentials that ranged between -40 and -75 mV. Fig. 1 *A* shows an experiment in which the cell membrane potential was recorded
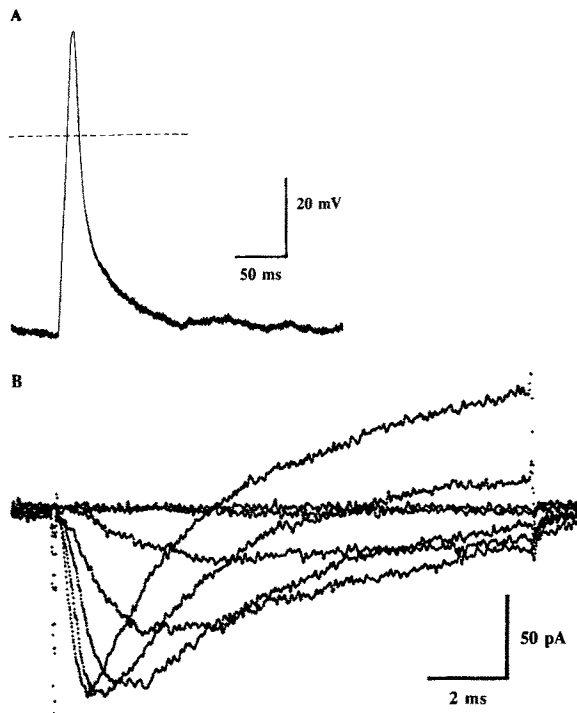

FIGURE 1. (*A*) Action potential recorded from an undifferentiated cell. The dashed line indicates 0 mV. The stimulus (not shown) was 20 ms in duration and of sufficient magnitude to depolarize the resting cell by 10–20 mV. The pipette contained potassium solution 1 and the experiment was performed at 21°C. (*B*) A family of membrane currents recorded from an undifferentiated cell at 18°C with potassium solution 2 in the pipette. The cell was held at -80 mV and the test voltages ranged from -50 to 10 mV in steps of 10 mV. Each test pulse was preceded by a 50-ms prepulse to -100 mV.

using the current clamp mode of the patch clamp amplifier. The cell's intrinsic resting potential was measured as -45 mV. A holding current sufficient to increase the resting potential to -50 mV was applied. Current pulses of sufficient magnitude to depolarize the cell membrane potential passively by 10–20 mV were delivered through the patch pipette to elicit action potentials. Action potential overshoots were typically 20–25 mV and the maximum rate-of-rise ($\dot{V}_{max}$) was ~ 10 V/s. The value of $\dot{V}_{max}$ is quite low compared with typical adult neurons ($> 10^3$ V/s) and reflects the low density of sodium channels in the surface membrane of undifferentiated LA-N-5 cells (see Table I).

Fig. 1 B shows a family of whole-cell currents recorded from an undifferentiated LA-N-5 cell with a potassium-containing solution (pipette solution 2) in the patch pipette. The cell was held at −80 mV and depolarized to test voltages from −50 to +10 mV for 12 ms. The test pulse was preceded by a prepulse to −100 mV for 50 ms to remove inactivation. Both inward and outward membrane currents were elicited within the range of membrane voltages applied. Inward current activated at a membrane voltage between −50 and −40 mV, and reached maximum amplitude within less than a millisecond at −10 to 0 mV. It is also apparent that the rates of inward current activation and inactivation increased as the test voltages became more positive. The waveform and voltage dependence of the traces suggest that the inward current is a sodium current. At positive test potentials, a delayed outward current was also activated. Outward current could be blocked by 5–10 mM extracellular TEA (data not shown) or by substituting cesium for potassium in the pipette solution (compare Fig.1 B with Figs. 3 and 7), which suggests that it is a potassium current (see also Weiss et al., 1990a). A cesium pipette solution was routinely used in the experiments described below to give recordings of the sodium current without contamination by outward currents.

A graph of peak inward current versus voltage from an undifferentiated LA-N-5 cell is shown in Fig. 2. The maximum current was recorded at a membrane potential of 0 mV, and the current reversed at +66.5 mV. The reversal potential was determined by interpolation of the data points within the voltage range of +30 to +90 mV. The average reversal potential obtained from six cells was +68.2 ± 3.1 mV (mean ± SD), which is quite close to the calculated Nernst potential for sodium, $E_{Na} = +66.7$ mV at 18°C, suggesting that the inward current is sodium ion selective. Further support for the identity of the inward current came from pharmacological experiments. Inward current could be completely blocked by the sodium channel–specific neurotoxin, TTX. As will be elaborated below, the concentration of TTX required for complete block was quite high, >15 μM, which is attributed to the presence of TTX-resistant sodium currents. High-threshold (L-type) calcium channels, although present in LA-N-5 cells (Weiss et al., 1990b), exist at a very low surface density and did not contribute measurably to the inward currents recorded in the experimental conditions reported here. Low-threshold (T-type) calcium channels have not been detected in LA-N-5 cells, even in the presence of 50 mM $BaCl_2$ (data not shown). Therefore, under physiological conditions TTX-blockable sodium current was the only measurable inward current.

The voltage dependence of inactivation of the sodium current was measured by the classical method of applying a constant test pulse from prepulses of varying amplitudes and calculating the Hodgkin-Huxley inactivation parameter h_∞ (Hodgkin and Huxley, 1952). Fig. 2 B shows a plot of h_∞ versus prepulse voltage from an undifferentiated neuroblastoma cell. Experimental data have been plotted as symbols. The voltage at which half of the sodium current was inactivated, $V_{1/2}$, was determined by a least-squares, nonlinear fitting of the data according to the equation

$$h_\infty(V) = I_{Na}/I_{Na,max} = 1/\{1 + \exp[(V_{pp} - V_{1/2})/a_h]\} \tag{2}$$

where V_{pp} is the prepulse voltage and a_h is the steepness of the voltage dependence. $V_{1/2}$ was −50.7 mV and a_h was 9.8 for the data shown in Fig. 2 B. The average $V_{1/2}$ for

six cells was −46.3 ± 4.8 mV (mean ± SD). Thus, at the normal resting potential of these cells approximately half of the sodium channels are available for activation. The activation and inactivation characteristics, pharmacology, and reversal potential of the inward current, and the apparent absence of other inward currents suggest that the rapid depolarization phase of the action potential in these neuroblastoma cells is dominated by sodium conductance.

Components of Sodium Current

One of the first observations that different kinds of sodium channel coexist in one type of cell came from studies of the TTX sensitivity of action potentials in
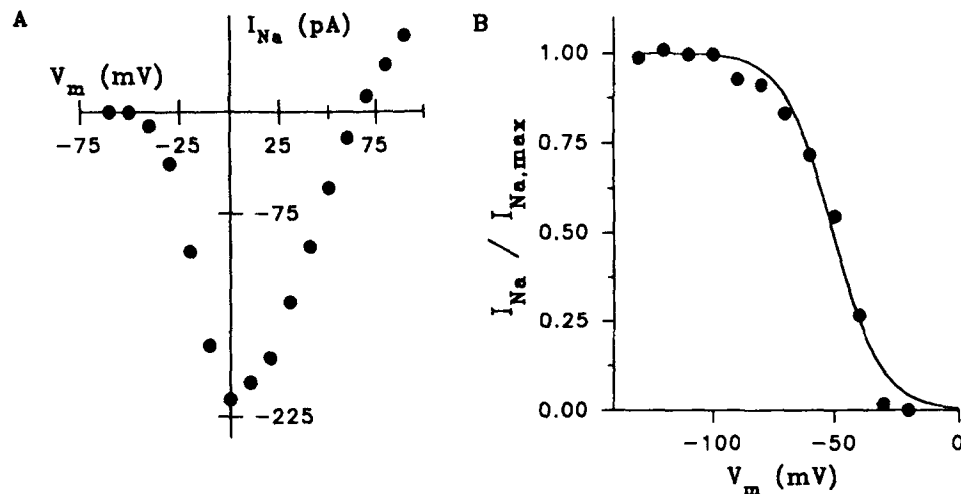

Figure 2. (*A*) Peak sodium current versus membrane voltage from an undifferentiated LA-N-5 cell at 18°C. The cell was held at −70 mV and each 8-ms test pulse was preceded by a 50-ms prepulse to −110 mV. The reversal potential, determined by interpolation, is E_{Na} = +66.5 mV. (*B*) Inactivation of sodium current relationship for an undifferentiated LA-N-5 cell at 18°C. The cell was held at −80 mV. Test pulses to −10 mV and 10 ms in duration were applied after 50-ms prepulses which varied in amplitude between −130 and −20 mV. Experimental data are plotted as symbols and the smooth curve represents a fit of Eq. 2 to the data. The $V_{1/2}$ was −50.7 mV.

developing muscle (Harris and Marshall, 1973). TTX remains a most useful pharmacological tool to distinguish different forms of functional sodium channels. It was used in this study to show that LA-N-5 cells express TTX-sensitive and TTX-resistant sodium currents. Fig. 3 *A* shows an experiment in which two different doses of TTX were used to separate pharmacologically the two types of sodium current. The first dose of 25 nM TTX reduced the current to ∼39% of control (Fig. 3 *A*, middle trace). Using the following equation for the equilibrium dissociation constant (K_d) in which $I_{Na,max}$ is the sodium current recorded in the absence of TTX,

$$K_d = I_{Na} * [TTX]/(I_{Na,max} - I_{Na}) \tag{3}$$

the apparent K_d calculated from the control and middle experimental traces was 16 nM. When the concentration of TTX was increased to 2.5 μM, the sodium current decreased further to ~10% of the control amplitude (Fig. 3 A, top trace). Assuming once again a single binding affinity of sodium channels for TTX, the apparent K_d calculated from the control and top traces of Fig. 3 A was 278 nM. The two apparent
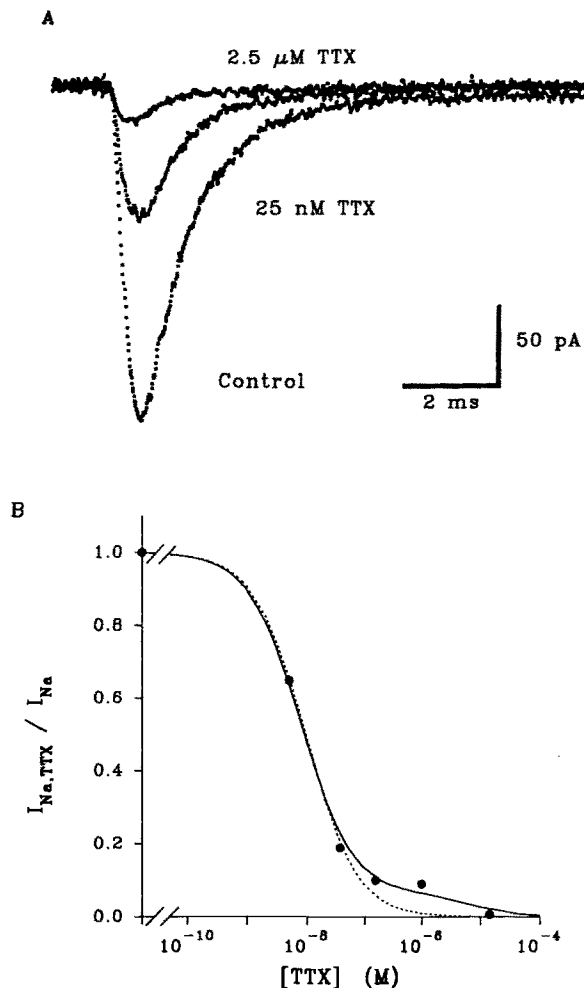
A

FIGURE 3. (A) The effects of two doses of TTX on sodium currents recorded from an undifferentiated cell at 18°C with cesium pipette solution. Voltage steps were identical for all three traces. The cell was held −80 mV. Test pulses to 0 mV were preceded by 50-ms prepulses to −110 mV. (B) A dose–response curve generated for five doses of TTX from an undifferentiated LA-N-5 cell at 18°C. The smooth curve represents a fit of a two-site binding model to the data points (see Eq. 1). The equilibrium dissociation constants (K_d) obtained from the curve fit were 7.8 nM and 6.4 μM, with the low affinity binding site comprising 7% of the total current. The broken line represents the best fit of a one-site binding model (Eq. 3) to the data, which yielded a K_d of 9.5 nM.

K_d's differ by a factor of 17, which provides clear evidence that sodium channels with more than one affinity for TTX were present in this LA-N-5 cell.

Sequential application of five doses of TTX ranging from 5 nM to 14 μM generated the dose–response relation in the experiment represented in Fig. 3 B. The experimental data (symbols) were best fit by a two-site binding model described by Eq. 1 (see Methods) and the parameters obtained from the fit were used to generate the smooth curve. For comparison, the best fit of the data to a one-site model described by Eq. 3 is also shown in Fig. 3 B as a broken line. Although the one-site

model fit the current amplitudes well at low concentrations of TTX, it did not predict the current remaining at micromolar TTX concentrations. The equilibrium K_d's obtained from the fit of the two-site model were $K_{d,TS} = 7.8$ nM and $K_{d,TR} = 6.4$ μM for TTX-sensitive and TTX-resistant sodium currents, respectively. These values are similar to those from whole-cell current measurements made on rat myoballs from primary cultures at 20°C; i.e., 13 nM and 3.2 μM (Gonoi et al., 1985).

To distinguish between the properties of TTX-sensitive and TTX-resistant sodium currents in the studies described in the following section, sodium currents were recorded in the absence and presence of a concentration of TTX calculated to block nearly all of the TTX-sensitive but very little of the TTX-resistant sodium current. The K_d's obtained from the dose–response experiment in Fig. 3 B were substituted individually into Eq. 3 to calculate that a concentration of 160 nM TTX would block >0.95 of the TTX-sensitive current, but <0.025 of the TTX-resistant current. In a few experiments, 210 nM TTX was used.

Properties of TTX-resistant Sodium Current

Current–voltage relationships for total and TTX-resistant sodium current from an undifferentiated LA-N-5 cell are shown in Fig. 4 A. The TTX-resistant current is plotted both at its absolute amplitude and scaled so that the peak amplitude (at −10 mV) is the same as the peak total sodium current (at 0 mV). The activation of TTX-resistant current was shifted toward more negative voltages by approximately 20 mV. In the experiment shown, the current measured at the membrane potential Vm = −50 mV was of equal magnitude both in the absence and presence of 160 nM TTX, indicating that, for small depolarizations, nearly all of the inward current was carried by TTX-resistant sodium channels. In seven similar experiments, TTX-resistant current comprised 91 ± 17% (mean ± SD) of the total sodium current measured at −50 mV.

The normalized sodium conductance versus voltage relationships in the absence and presence of TTX, calculated as $g_{Na} = I_{Na}/(V_m - E_{Na})$ where V_m is the applied membrane voltage, are represented by filled symbols in Fig. 5, A and B. In the experiment shown, the activation of half-maximal conductance of TTX-resistant sodium current was shifted to more negative voltages by 16.8 mV relative to the total sodium conductance (measured in the absence of TTX). In seven experiments the mean shift of TTX-resistant conductance relative to total conductance was 12.5 ± 4.0 mV. The TTX-sensitive component of the total sodium conductance was calculated by subtracting TTX-resistant from total sodium conductance for the data in Fig. 5, A and B, and plotted as normalized conductance versus voltage in Fig. 5 C. Removing the contribution of TTX-resistant conductance from the total sodium conductance flattens the foot of the activation curve. In some cells there was also a slight shift of the voltage at which half-maximal activation occurs. The mean shift between the half-maximal activation voltages for TTX-resistant and TTX-sensitive conductance in six cells was 13.8 ± 4.9 mV (mean ± SD). This result is consistent with the proportionally large contribution of TTX-resistant current to the total current for small depolarizations, and the small contribution for large depolarizations.

The voltage dependence of inactivation of sodium current was determined as described above in the absence and presence of TTX. Fig. 4 B shows plots of h_∞

versus prepulse voltage from an undifferentiated neuroblastoma cell in the absence and presence of 210 nM TTX. Experimental data are plotted as symbols. The smooth curve, fit to Eq. 2, yielded $V_{1/2}$ values of -46.0 and -70.4 mV, respectively, for total and TTX-resistant current. The mean $V_{1/2}$ measured for 12 cells in the absence of TTX was -46.1 ± 7.2 mV (mean $\pm$ SD). The mean $V_{1/2}$ for the eight cells measured in the presence of 160 TTX was -77.0 ± 8.8 mV. The h_∞ versus voltage relationships are also plotted (open symbols) in Fig. 5 with the conductance
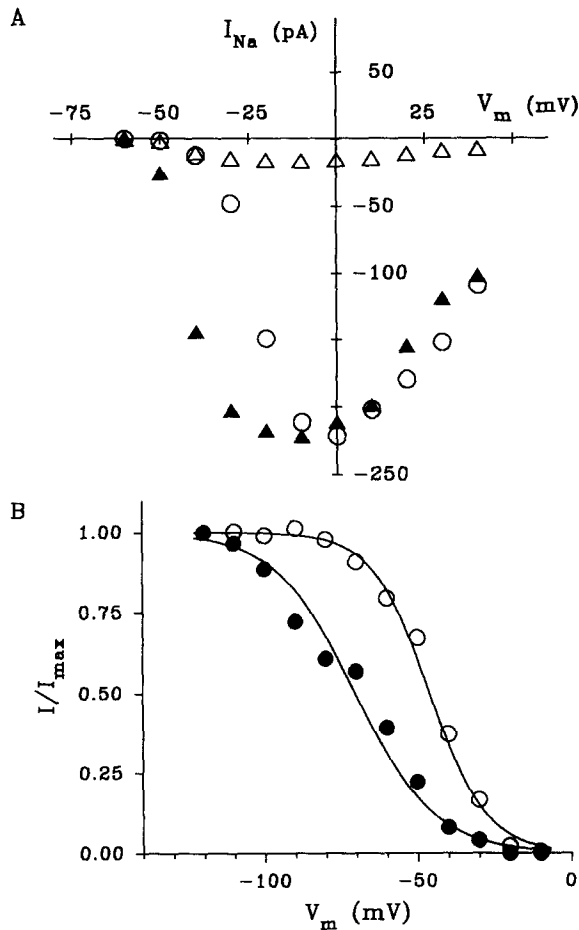

FIGURE 4. (A) Current–voltage relationship in the absence (*open circles*) and presence of 160 nM TTX (*triangles*) at 18°C. TTX-resistant sodium currents are plotted at their originally recorded amplitudes (*open triangles*) and scaled so that the peak TTX-resistant and total currents are equal (*filled triangles*). The cell was held at -80 mV and test pulses were preceded by 50-ms prepulses to -110 mV. (B) The steady-state inactivation (h_∞) relationship measured in the absence (*open circles*) and presence (*filled circles*) of 210 nM TTX at 18°C. The smooth curves lines represent fits to Eq. 2 (see text) from which the half-inactivation voltages were $V_{1/2} = -46.0$ and -70.4 mV in the absence and presence of TTX, respectively. The steepness values were $a_h = 9.3$ and 13.0, respectively. The cell was held at -80 mV and pulsed to the indicated voltage (V_m) for 50 ms preceding the test pulse to 0 mV.

activation curves to show the voltage range (window) in which a net stationary sodium conductance (window current) could occur. The window current voltage range was shifted by about -20 mV for TTX-resistant relative to total sodium current. The magnitude of the voltage range that includes the window current was slightly greater for the TTX-resistant current. When the total and TTX-resistant conductances were subtracted to give specifically the TTX-sensitive conductance, as shown in Fig. 5 C, the window current was reduced, since the TTX-resistant current contributes signifi-

A

Control

B
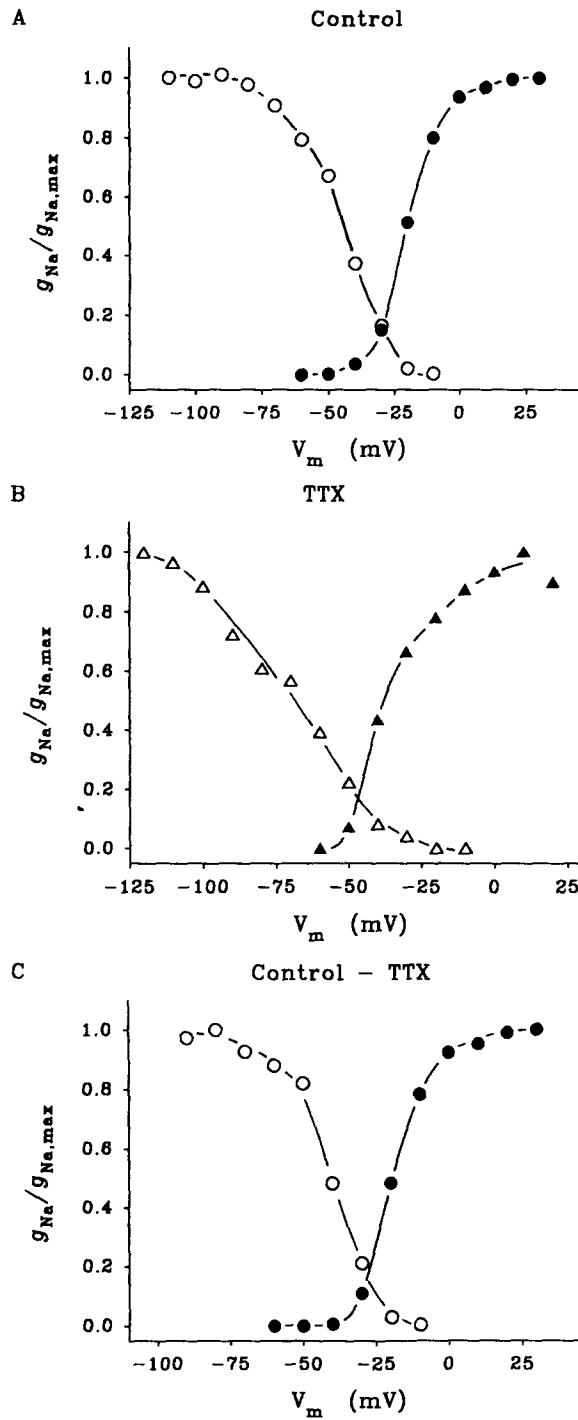
TTX

C

Control − TTX

FIGURE 5. Activation and inactivation of normalized sodium conductance calculated from the data shown in Fig. 4. The area of positive conductance common to both curves in each panel represents the voltage range were persistent (window) sodium currents can occur. Curves through the data points are drawn by eye. (*A*) Conductance calculated from total sodium current recorded in the absence of TTX. (*B*) Conductance calculated from sodium current recorded in the presence of TTX (see legend to Fig. 4 and text for further explanation). (*C*) Conductance calculated for the difference current measured in the presence and absence of TTX.

cantly to the current measured near the foot of the activation curve but has little effect on the h_∞ curve, which was generated with a test voltage of 0 mV.

Effects of Retinoic Acid–induced Differentiation on Sodium Channel Properties

A TTX dose–response experiment similar to that shown in Fig. 3 *B* was repeated on a differentiated LA-N-5 cell to determine whether the toxin-binding affinities of the two types of sodium channels remained constant after differentiation by retinoic acid. The result is shown in Fig. 6. As in Fig. 3 *B*, the continuous curve is a fit of the data to a two-site binding model described by Eq. 1 and the broken line is a fit of the same data to a one-site binding model described by Eq. 3. The two-site model gave the best fit, although the difference between the fits of one- and two-site models now appears less dramatic than for the undifferentiated cell (Fig. 3 *B*) because there is proportionally less TTX-resistant current in the differentiated cell. The change in proportions of
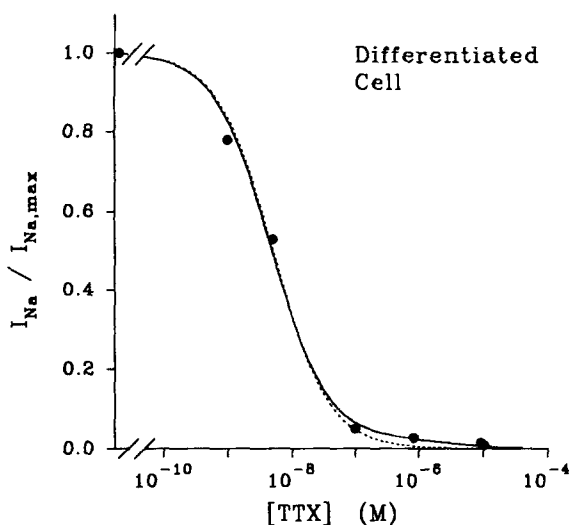

FIGURE 6. Dose–response curve generated for five doses of TTX from a differentiated LA-N-5 cell at 18°C. The smooth curve represents a fit of a two-site binding model to the data points (see Eq. 1). The equilibrium K_d's obtained from the curve fit were 4.6 nM and 3.5 μM, with the low affinity binding site comprising 2.5% of the total current. The broken line represents the best fit of a one-site binding model (Eq. 3) to the data, which yielded a K_d of 5.0 nM.

the two types of sodium current is described in more detail below. The equilibrium K_d's obtained from the fit of the two-site binding model to the data were $K_{d,TS}$ = 4.6 nM and $K_{d,TR}$ = 3.5 μM for TTX-sensitive and TTX-resistant sodium currents, respectively. These values are similar to those obtained from the undifferentiated cell (Fig. 3 *B*) and also to published values from muscle preparations (e.g., Gonoi et al., 1985). The dose–response experiments indicate that during differentiation there is no change in the affinity of sodium channels for TTX in this human neuroblastoma cell line.

The voltage dependence of activation and inactivation were also unchanged after retinoic acid–induced differentiation. The proportion of inward current at −50 mV was composed of >85% TTX-resistant sodium current (two cells), indicating that TTX-resistant sodium channels in differentiated cells also open at more negative voltages than TTX-sensitive sodium channels. Experiments to detect calcium cur-

rents indicated that calcium currents are not detectable in differentiated LA-N-5 cells bathed in physiological saline. Steady-state inactivation (h_∞) in differentiated cells was also not significantly changed by differentiation. The half-inactivation voltage for total sodium current was $V_{1/2} = -47.9 \pm 8.3$ mV $(n = 8)$ and for TTX-resistant current -82.5 ± 8.7 mV $(n = 6)$, which indicates a shift similar to that observed in undifferentiated cells.

Effects of Retinoic Acid–induced Differentiation on Sodium Channel Density

To enable rapid determination of the relative amounts of TTX-sensitive and TTX-resistant sodium current in undifferentiated and differentiated LA-N-5 neuroblastoma cells, sodium currents were recorded in the absence and presence of 160 nM TTX. Sodium current recorded from individual cells before and after perfusion of TTX into the experimental chamber permitted computation of the mean ratio per cell of TTX-resistant to total sodium current (see below and Table I). In many of the cells studied, cell capacitance was determined and the measurements of sodium currents were normalized to the individual cell capacitance. This protocol was used to obtain data that could be used to eliminate the bias that might be introduced by variable cell size, since differentiation of LA-N-5 cells causes neurite outgrowth and an overall increase in cell membrane area. In all experiments on differentiated cultures, cells were selected for small diameter and limited neurite extensions. The capacitance measurements (see Table I) suggest that this selection by visual examination produced similar populations of cells with respect to membrane area, since the mean capacitance for undifferentiated and differentiated cells was 20 and 24.1 pF, respectively.

Fig. 7 *A* shows current records from four cells which had sodium current surface densities (sodium current normalized to cell capacitance) representative of the mean values of total and TTX-resistant current calculated from the pooled data from all cells before and after differentiation (Table I). There was a distinct increase in the surface density of total but not TTX-resistant sodium current after retinoic acid–induced differentiation. Comparison of the mean total sodium current values, measured before and after differentiation $(I_{\mathrm{Na,Total}}$ in columns 1 and 2 of Table I), indicates a 3.6-fold increase in the magnitude and a 2.3-fold increase in the surface density. The difference for both current magnitude and density was significant when tested with Wilcoxon's rank sum test $(P < 0.002$ for magnitude and $P < 0.05$ for density), which was used here because of the nonnormal distribution of the data as shown in Fig. 7, *C* and *D* (see Methods). The analysis of these results indicates, therefore, that the increase in sodium current in LA-N-5 cells after differentiation was not related to cell size. The effects of retinoic acid–induced differentiation on TTX-resistant current were a twofold increase in current magnitude and almost no change (1.1-fold increase) in current density, neither of which was significant as determined by the rank sum test.

The data given above indicate that retinoic acid–induced differentiation of LA-N-5 cells induces the expression of functional TTX-sensitive sodium channels, which is specific with respect to TTX-resistant sodium channels. The contribution of TTX-sensitive current to the total current was, respectively, >80% and 90% of the total sodium current before and after differentiation. By simple algebraic manipulation of
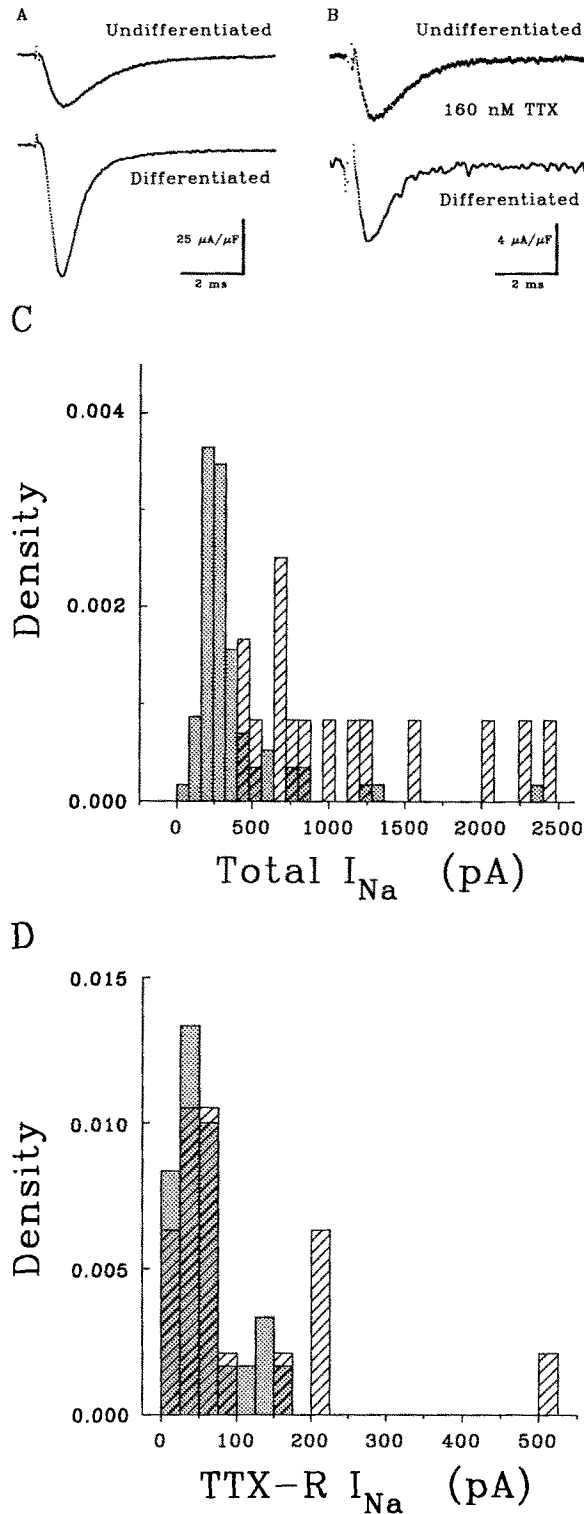
FIGURE 7. (A and B) Sodium currents recorded from LA-N-5 cells before and after differentiation induced by retinoic acid and cyclic AMP, and in the presence and absence of 160 nM TTX. The traces were selected to approximate the mean values given in Table I. All records shown in A and B were recorded with cesium solution in the pipette. (A) Total sodium current in cells before and after differentiation. Cells were held at −80 mV and depolarized to 0 mV from a 50-ms prepulse to −110 mV. (B) TTX-resistant sodium current before and after differentiation. The same voltage conditions were used as in A, except that the prepulse was to −130 mV. All traces were recorded at 18°C with pipette solution 3. (C and D) Amplitude histograms of total and TTX-resistant sodium current magnitudes before (stippled bars) and after differentiation (hatched bars) as described above. The ordinates, given as density, represent the number measurements within the limits of the bin width, normalized to give a total distribution area equal to one.

the means in Table I, TTX-sensitive sodium current magnitude and density increased, respectively, by 4- and 2.6-fold after differentiation.

From the increase in total, but not TTX-resistant, sodium current, a decrease in the ratio of TTX-resistant to total sodium current estimated from individual cells should also be expected. The data in Table I show that the mean of ratios determined from individual cells decreased from 0.15 to 0.09 after retinoic acid–induced differentiation, and this change was significant by the rank sum test ($P = 0.005$). The ratio of TTX-resistant to total sodium current can also be calculated from the pooled data from all cells. These data include measurements of TTX-resistant sodium current recorded from cells exposed to TTX before being patch clamped, and thus provide the control that the TTX-resistant current obtained after a period of recording in TTX-free solution had not suffered "run down" during the (typically) 20–30-min experiments. The differences between the ratio of TTX-resistant to total sodium currents before and after differentiation calculated from the means of total and TTX-resistant currents in Table I are slightly greater than the mean difference of ratios determined from individual cells.

DISCUSSION

There are three principal findings of this paper. (*a*) The LA-N-5 human neuroblastoma cell line, which acquires adult neuronal characteristics when treated with retinoic acid, is excitable in its proliferative, undifferentiated state, and the excitability is dependent upon the presence of two types of sodium channels, measured as TTX-sensitive and TTX-resistant sodium current. (*b*) TTX-resistant sodium channels have voltage-dependent activation and inactivation, which is shifted in the direction of negative voltages so that its window of steady-state activity is near the intrinsic cell resting potential. (*c*) Retinoic acid–induced differentiation stimulates a >2.5-fold increase in the density of TTX-sensitive sodium current in the surface membrane, and this increase is statistically significant. However, differentiation has no discernible effect on equilibrium K_d's for TTX block of the sodium channels, nor on the voltage sensitivity of activation or inactivation. These results are discussed below with regard to the role of sodium channels in the excitability of developing nerve and muscle cells, and the regulation of sodium channel expression in excitable cells.

LA-N-5 cells are excitable in their undifferentiated state, a result that has been reported for a high percentage of murine neuroblastoma clones, some of which exhibit spontaneous action potentials (Nelson et al., 1971; Peacock et al., 1972; Kimhi, 1981). The excitability of LA-N-5 cells depends on sodium currents, which have been shown in this paper to be composed of two components separable by their sensitivity to block by TTX. The sodium channels with a low affinity for TTX were also distinguished by a shift of the voltage dependence of activation and inactivation of −10 to −30 mV. The voltage range in which a window current occurs, i.e., where sodium channels open but are not completely inactivated, is within the range of resting potentials from −40 to −70 mV measured in LA-N-5 cells. These results suggests that TTX-resistant channels could be the principal inward current during the early depolarization phase of action potentials. In muscle, TTX-resistant sodium channels have voltage-dependent properties of activation and inactivation similar to those described in this paper (Pappone, 1980; Weiss and Horn, 1986*a*; Gonoi et al.,

1989; Weiss, 1990). Involvement of sodium channels in initiating action potentials has been proposed for spontaneous action potentials that occur in developing and denervated skeletal muscle and are correlated with the presence of TTX-resistant sodium channels (Harris and Marshall, 1973; Purves and Sackmann, 1974).

In a variety of models of developing excitable cells, including neonatal rat dorsal root ganglion, rat PC12, and rat skeletal muscle cells, TTX-resistant sodium currents are present at the stage when the cells become excitable (Harris and Marshall, 1973; Kostyuk et al., 1981; Gonoi et al., 1985; O'Lague et al., 1985; Weiss and Horn, 1986a, b; Rudy et al., 1987). It is tempting to speculate that TTX-resistant channels may have been present in the spontaneously active murine neuroblastoma cells reported by Nelson et al. (1971). Excitability is not a uniform characteristic of undifferentiated neuroblastomas, as some cell lines are inexcitable and individual cells in excitable cell lines sometimes lack inward currents (Nelson et al., 1971; several cells in this study). The PC12 clonal cell line, frequently used as a model for neuronal differentiation, is inexcitable in its undifferentiated state.

There was a more than twofold increase in sodium current density, from 24.9 to 57.8 $\mu A/\mu F$, in the LA-N-5 neuroblastoma cells differentiated with retinoic acid in the experiments reported here. The increase in sodium current was accounted for by upregulation of TTX-sensitive sodium channels, since the TTX-resistant sodium current density, which was measured specifically in the presence of TTX, increased by a statistically insignificant amount (from 4.5 to 5.1 $\mu A/\mu F$). Upregulation of TTX-sensitive sodium channel density during differentiation or maturation is probably common to most excitable cells that develop sodium-dependent action potentials, and has been reported in studies of muscle and many central nervous system cells (see, for example, Kostyuk et al., 1981; Sherman and Catterall, 1982; Huguenard et al., 1988; Yarowsky and Krueger, 1989). The majority of these studies indicate that TTX-resistant sodium channels, if they are present, are not coregulated with TTX-sensitive sodium channels. However, in rat PC12 cells, TTX-resistant sodium channels are only detectable after NGF-induced differentiation, which also greatly increases the density of TTX-sensitive channels and induces electrical excitability (Rudy et al., 1982, 1987; O'Lague et al., 1985). The effect of NGF on TTX-sensitive sodium channel expression has recently been shown by Kalman et al. (1990) to be mediated by cyclic AMP-dependent protein kinase. A similar result was shown previously in developing skeletal muscle by Sherman et al. (1985), in which it was determined that the effect of cyclic AMP on sodium channels is specific to TTX-sensitive over TTX-resistant sodium channels. Regulation of the two types of sodium channels via separate pathways is also strongly supported by numerous studies of developing skeletal muscle where TTX-resistant sodium channels disappear with age and after innervation, while TTX-sensitive channel density increases (see for example, Sherman and Catterall, 1982; Gonoi et al., 1985; Weiss and Horn, 1986a, b). The results reported here on LA-N-5 cells support a hypothesis of separate regulatory pathways and do not discount the possibility that cyclic AMP may be a common stimulus of TTX-sensitive sodium channel expression in most excitable cells.

Neuronal TTX-sensitive sodium channels are thought to be encoded by any of at least three different mRNAs and have been labeled types I, II, and III (Noda et al., 1986; Auld et al., 1988). The type of TTX-sensitive sodium channel that is expressed

in adult peripheral nerve has been proposed to be type II (Stühmer et al., 1987). During early development other forms of TTX-sensitive sodium channels may be present, however. For comparison, in developing rat brain the levels of expresssion of mRNA for the three sodium channel types have different temporal and regional patterns (Beckh et al., 1989). The finding that channel subtype distribution changes during development in brain presents the alternative possibilities that the increase in TTX-sensitive sodium channel expression during differentiation in peripheral neurons represents either upregulation of a single type of TTX-sensitive channel, or the promotion of a previously silent sodium channel gene. Since electrophysiological differences between the three types of TTX-sensitive sodium channels have not yet been well defined, these possibilities will probably require other methods to be resolved.

REFERENCES

Auld, V. J., A. L. Goldin, D. S. Krafte, J. Marshall, J. M. Dunn, W. M. Catterall, H. A. Lester, N. Davidson, and R. J. Dunn. 1988. A rat brain Na channel alpha subunit with novel gating properties. *Neuron.* 1:449–461.

Barchi, R. L. 1988. Probing the molecular structure of the voltage-dependent sodium channel. *Annual Review of Neuroscience.* 11:455–495.

Beckh, S., N. Noda, H. Lubbert, and S. Numa. 1989. Differential regulation of three sodium channel messenger RNAs in the rat central nervous system during development. *European Molecular Biology Organization Journal.* 8:3611–3616.

Catterall, W. A. 1986. Molecular properties of voltage-sensitive sodium channels. *Annual Review of Biochemistry.* 55:953–985.

Dichter, M. A., A. S. Tischler, and L. A. Greene. 1977. Nerve growth factor-induced change in electrical excitability and acetylcholine sensitivity of a rat pheochromocytoma cell line. *Nature.* 268:501–504.

Diem, K., and C. Lentner. 1970. Scientific Tables. Ciba-Geigy Ltd., Basle, Switzerland. 192.

French, C. R., and P. W. Gage. 1985. A threshold sodium channel in pyramidal cells in rat hippocampus. *Neuroscience Letters.* 56:289–294.

Gilly, W. F., and C. M. Armstrong. 1984. Threshold channels: a novel type of sodium channel in squid giant axon. *Nature.* 309:448–450.

Gonoi, T., Y. Hagihara, J. Kobayashi, H. Nakamura, and Y. Ohizumi. 1989. Geographutoxin-sensitive and insensitive sodium currents in mouse skeletal muscle developing in situ. *Journal of Physiology.* 414:159–177.

Gonoi, T., S. J. Sherman, and W. A. Catteral. 1985. Voltage clamp analysis of tetrodotoxin-sensitive and -insensitive sodium channels in rat muscle cells developing in vitro. *Journal of Neuroscience.* 5:2559–2564.

Harris, J. B., and M. Marshall. 1973. Tetrodotoxin-resistant action potentials in newborn rat muscle. *Nature New Biology.* 243:191–192.

Hill, A. B. 1937. A Short Textbook of Medical Statistics. J. B. Lippincott Co., Philadelphia. 127–136.

Hodgkin, A. L., and A. F. Huxley. 1952. The dual effect of membrane potential on sodium conductance in the giant axon of *Loligo. Journal of Physiology.* 116:497–506.

Huguenard, J. R., O. P. Hamill, and D. A. Prince. 1988. Developmental changes in Na$^+$ conductances in rat neocortical neurons: appearance of a slowly inactivating component. *Journal of Neurophysiology.* 59:778–795.

Kalman, D., B. Wong, A. E. Horvai, M. J. Cline, and P. H. O'Lague. 1990. Nerve growth factor acts through cAMP-dependent protein kinase to increase the number of sodium channels in PC12 cells. *Neuron.* 2:355–366.

Kimhi, Y. 1981. Nerve cells in clonal systems. *In* Excitable Cells in Tissue Culture. P. G. Nelson and M. Lieberman, editors. Plenum Publishing Corp., New York, London. 173–245.

Kojima, H., H. Yawo, and M. Kuno. 1985. A low voltage-activated Na channel in the cockroach giant axon. *Journal of Physiological Society Japan.* 47:25a. (Abstr.)

Kostyuk, P. G., N. S. Veselovsky, and A. Y. Tsyndrenko. 1981. Ionic currents in the somatic membrane of rat dorsal root ganglion neurons. I. Sodium currents. *Neuroscience.* 6:2423–2430.

Llinas, R., and M. Sugimori. 1980. Electrophysiological properties of *in vitro* Purkinje cell dendrites in mammalian brain slices. *Journal of Physiology.* 305:197–213.

Machin, G. A. 1982. Histogenisis and histopathology of neuroblastoma. *In* Neuroblastoma. C. Pochedly, editor. Elsevier Biomedical, New York. 195–225.

Nelson, P. G., J. H. Peacock, T. Amano, and J. Minna. 1971. Electrogenesis in mouse neuroblastoma cells in vitro. *Journal of Cellular Physiology.* 77:337–352.

Noda, M., T. Ikeda, T. Kayano, H. Suzuki, H. Takeshima, M. Kurasaki, H. Takahashi, and S. Numa. 1986. Existence of distinct sodium channel messenger RNAs in rat brain. *Nature.* 320:188–192.

O'Lague, P. H., S. L. Huttner, C. A. Vandenberg, K. Morrison-Graham, and R. Horn. 1985. Morphological properties and membrane channels of the growth cones induced in PC12 cells by nerve growth factor. *Journal of Neuroscience Research.* 13:301–321.

Pappone, P. A. 1980. Voltage-clamp experiments in normal and denervated mammalian skeletal muscle fibres. *Journal of Physiology.* 306:377–410.

Peacock, J., J. Minna, P. Nelson, and M. Nirenberg. 1972. Use of aminopterin in selecting electrically active neuroblastoma cells. *Experimental Cell Research.* 73:367–377.

Purves, D., and B. Sakmann. 1974. Membrane properties underlying spontaneous activity of denervated muscle fibres. *Journal of Physiology.* 239:125–153.

Ritchie, J. M., and R. B. Rogart. 1977. The binding of saxitoxin and tetrodotoxin to excitable tissue. *Reviews of Physiology, Biochemistry, and Pharmacology.* 79:1–50.

Robson, J. A., and N. Sidell. 1985. Ultrastructural features of a human neuroblastoma cell line treated with retinoic acid. *Neuroscience.* 14:1149–1162.

Rudy, B., B. Kirschenbaum, and L. A. Greene. 1982. Nerve growth factor-induced increase in saxitoxin binding to rat PC12 pheochromocytoma cells. *Journal of Neuroscience.* 2:1405–1411.

Rudy, B., B. Kirschenbaum, A. Rubenstein, and L. A. Greene. 1987. Nerve growth factor increases the number of functional Na channels and induces TTX resistant Na channels in PC12 pheochromocytoma cells. *Journal of Neuroscience.* 7:1613–1625.

Sherman, S. J., and W. A. Catterall. 1982. Biphasic regulation of development of the high affinity saxitoxin receptor by innervation in a rat skeletal muscle. *Journal of General Physiology.* 80:753–768.

Sherman, S. J., J. Chrivia, and W. A. Catterall. 1985. Cyclic adenosine 3':5'-monophospate and cytosolic calcium exert opposing effects on biosynthesis of tetrodotoxin sensitive sodium channels in rat muscle cells. *Journal of Neuroscience.* 5:1570–1576.

Sidell, N., and R. Horn. 1985. Properties of human neuroblastoma cells following induction by retinoic acid. *Advances in Neuroblastoma Research.* 39–53.

Sidell, N., C. A. Lucas, and G. W. Kreutzberg. 1984. Regulation of acetylcholinesterase activity by retinoic acid in a human neuroblastoma cell line. *Experimental Cell Research.* 155:305–309.

Sonnenfeld, K. H., and D. N. Ishi. 1982. Nerve growth factor effects and receptors in cultured human neuroblastoma cell lines. *Journal of Neuroscience Research.* 8:375–391.

Stühmer, W., C. Methfessel, B. Sakmann, M. Noda, and S. Numa. 1987. Patch clamp characterization of sodium channels expressed from rat brain cDNA. *European Biophysical Journal.* 14:131–138.

Trimmer, J. S., and W. S. Agnew. 1989. Molecular diversity of voltage-sensitive Na channels. *Annual Reviews of Physiology.* 51:401–418.

Weiss, R. E. 1990. Coexistence of different types of sodium channels in striated muscle and nerve. *In* Transduction in Biological Systems. C. Hidalgo, J. Bacigalupo, E. Jaimovich, and J. Vergara, editors. Plenum Publishing Corp., New York. 261–274.

Weiss, R. E., C. J. Grantham, and M. B. Cannell. 1990*a*. Potassium channel control of repolarization in the human neuroblastoma cell line LA-N-5. *Biophysical Journal.* 57:112*a*. (Abstr.)

Weiss, R. E., M. A. Hediger, J. Hu, N. Sidell, and J. A. Talvenheimo. 1990*b*. The LA-N-5 human neuroblastoma cell line has L-type calcium channel mRNA similar to that found in skeletal muscle. *Biophysical Journal.* 57:306*a*. (Abstr.)

Weiss, R. E., and R. Horn. 1986*a*. Functional differences between two classes of sodium channels in developing rat skeletal muscle. *Science.* 233:361–364.

Weiss, R. E., and R. Horn. 1986*b*. Single-channel studies of TTX-sensitive and TTX-resistant sodium channels in developing rat muscle reveal different open channel properties. *Annals of the New York Academy of Science.* 479:152–161.

Weiss, R. E., and N. Sidell. 1989. TTX-sensitive and -resistant sodium channels in a human neuroblastoma cell line that differentiates in response to retinoic acid. *Society for Neuroscience Abstracts.* 15:537. (Abstr.)

Yarowsky, P. J., and B. K. Krueger. 1989. Development of saxitoxin-sensitive and insensitive sodium channels in cultured neonatal rat astrocytes. *Journal of Neuroscience.* 9:1055–1061.